

A Method for the Detection of the Distance & Orientation of the Relief Well to a Blowout Well in Offshore Drilling

Cui Li¹, Deli Gao¹, Zhiyong Wu¹ and Binbin Diao¹

Abstract: At present, a relief well is the most reliable method to control serious blowout accidents, and it is necessary to detect very accurately the relative position of the relief well and the blowout well. The detection tool should be capable of detecting directly the relative distance and direction between the relief well and the blowout well. Its detection accuracy should also meet the engineering demand of drilling a relief well. Using the working principle of a proposed detection tool, this paper analyzes the spread and attenuation laws of the current injected by a single-electrode or three-electrode array in the relief well. The present paper also considers the casing of the blowout well, and then develops a model for the distribution of the alternating magnetic field generated by the current in the blowout well casing, and lastly confirms the method of computation of the relative distance and orientation of the relief well to blowout well. The results of the present research can also be used as theoretical foundations for developing the guidance tool for the directional drilling of the relief well.

Keywords: relief well; blowout well; detection tool; single-electrode; three-electrode array; alternating magnetic field

1 Introduction

In recent years, many oil leakage accidents which occurred on the offshore drilling platforms have caused serious ecological disasters. The concept of a relief well is still the most reliable method to control serious blowout accidents [Guo, Ji and Tang (2010)], and it is necessary to detect the relative position of the relief well and blowout well accurately. At present, some companies generally use a Wellspot tool to drill the relief well into the blowout well.

Because the well-head of the blowout well is usually under dangerous conditions,

¹ State Key Laboratory of Petroleum Resource and Prospecting, China University of Petroleum, Beijing102249, China. Corresponding author: Deli Gao. E-mail: gaodeli@cup.edu.cn; licui1219@163.com

detection devices of the traditional electromagnetic ranging guidance systems, such as the Rotating Magnet Ranging Service System, and the Magnetic Guidance Tool can't be located in the blowout well [Wang and Gao (2008); Diao and Gao (2011a)]. However, the detection device of Wellspot tool can be located in the relief well, so it can directly detect the relative distance and direction from the relief well to the blowout well [Leraand, Wright and Zachary (1990); Grace, Kuckes and Branton (1988); Kuckes, Hay and McMahon (1984)]. However, the key technologies of the Wellspot tool are still confidential and monopolistic. In this paper, the working principles of the downhole detection tools, based on the single-electrode and the three-electrode array, are discussed, and the method of computation of the relative distance and direction from relief well to blowout well is presented. The presently reported research results can be used as theoretical foundations for developing the tools for directional drilling guidance of the relief well.

2 Working principle of the detection tool

As shown in Fig.1, the detection tool for connecting the relief well to the blowout well mainly includes an alternating current (A.C.) source, the surface electrode, the downhole electrode including a single-electrode and a three-electrode array, the sensor, and the computational software [Morris, Walters and Costa(1971)].

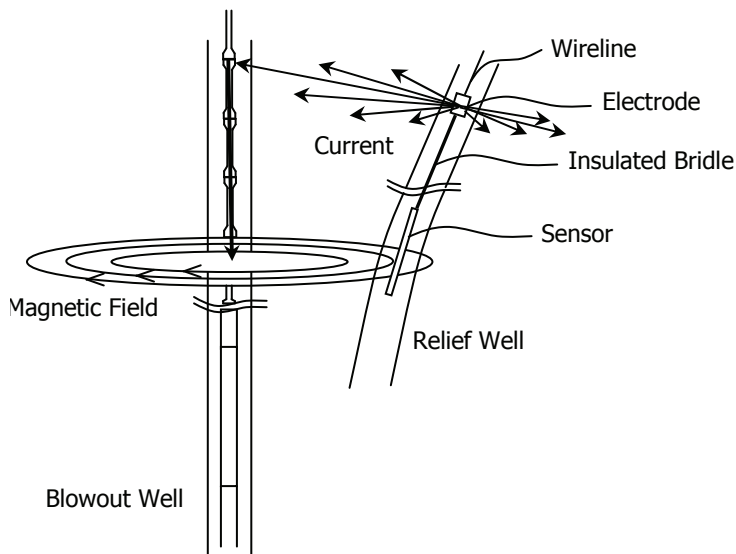


Figure 1: Working principle of the detection tool

The surface electrode is located near the well-head of the relief well, and the down-

hole electrode and the sensor are connected by the insulated bridle. The A.C. source provides low-frequency alternating current to the downhole electrode, which contacts the earth-formation surrounding the relief well and injects the current into the earth-formation, then the current will flow in a spherically symmetric way into the earth-formation. Since the casing and the drill pipe in the blowout well have much higher conductivity than the earth-formation, the current injected into the earth will concentrate on the casing or drill pipe and flow upwardly and downwardly along the casing or drill pipe. According to the Ampere's law, a portion of that current flowing downwardly will produce an alternating magnetic field around the casing which will be detected by the sensor [Bruist (1971); Arnwine and Ely (1977)]. Meanwhile, the magnetic field at the sensor generated by the current injected by the downhole electrode is zero, it has no effect on the weak signal detected by the sensor. In the measurement, the sensor must be static, otherwise, the rotation and vibration of the sensor would make the measurement of the small, low-frequency magnetic field impossible [Kuckes, Cornell and Ritch (1983)].

The technological advantages of the detection tool are as follows: 1) this detection tool could directly detect the relative distance and orientation of the relief well to the blowout well, which could avoid the drawback with the traditional MWD which generates cumulative errors with increasing well-depths, 2) the signal source and the signal detector of this detection tool are located in the relief well, so that it is suitable for the working conditions that the well-head of blowout well is very dangerous, 3) this detection tool has a larger detection range, and its limits on working temperature could be 200°C, so that it can be used for deep well connections [Diao and Gao (2011b)].

Although this detection tool has so many advantages, it can't be used for measurements while drilling. In each measurement, workers need to take the drilling bit and the drill pipe out of hole, and then run this detection tool, which will greatly increase the drilling time. Therefore, the detection tool for connecting relief well to blowout well is generally used for drilling the relief well only, and can't be applied in other working conditions, such as an anti-collision of cluster well.

3 Spread and attenuation law of the alternating current

Under following three assumptions: 1) the formation is uniform and its conductivity is given by σ_e , 2) the casing has an infinite length, 3) the radius of casing is given by r_c , which is much smaller than the current-injection-electrode-to-casing-axis radius, R , so that the casing in the blowout well can be replaced by a circular column of the formation, which has the same resistance per unit length. The radius

of this circular column of the formation can be expressed as

$$r_e = \sqrt{\frac{2\sigma_c}{\sigma_e} r_c h_c} \quad (1)$$

Where σ_c is the conductivity of casing, h_c is the casing wall thickness. The metal casing has obvious short-circuiting effect on the parallel component of current flow in its vicinity, so the sensitivity of the sensor is such that an AC magnetic induction of less than 0.01nT can be detected. This corresponds to the magnetic field generated by a current of 2mA on the blowout well casing 30m away [Kuckes, Cornell and Ritch (1983); Kuckes (1982)].

3.1 Current injected by a single-electrode

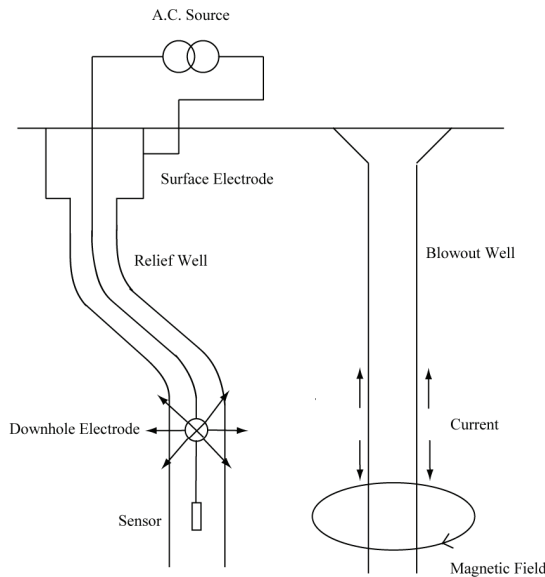


Figure 2: Working principle of the detection tool based on single-electrode

As shown in Fig. 2, a single-electrode can be similar to a point DC current source, whose emission current is the uniform distribution in the space orientation, and the electric field at infinity will decay to zero [Chen and Zhao (2009)]. If the current injected by single-electrode is given by I_0 , the current density j_0 generated by single-electrode at any point a distance of R away can be expressed as

$$j_0 = \frac{I_0}{4\pi R^2} \quad (2)$$

Noting that the electric field E_{01} and the current density j_0 in the earth are related by $j_0 = \sigma_e E_{01}$, the electric field is given by

$$E_{01} = \frac{I_0}{4\pi\sigma_e R^2} \quad (3)$$

As shown in Fig. 3, in view of the radius of circular column of earth, r_e , the current on the casing in the blowout well is given by [Kuckes, Cornell and Ritch (1983); Kuckes (1982)]

$$I_{\rho 1} = \int \vec{j}_0 \cdot d\vec{s} = \int \sigma_e E_{01} ds = \sigma_e \cdot 2\pi r_c h_c E_{01} = \frac{r_e^2}{4R^2} I_0 \quad (4)$$

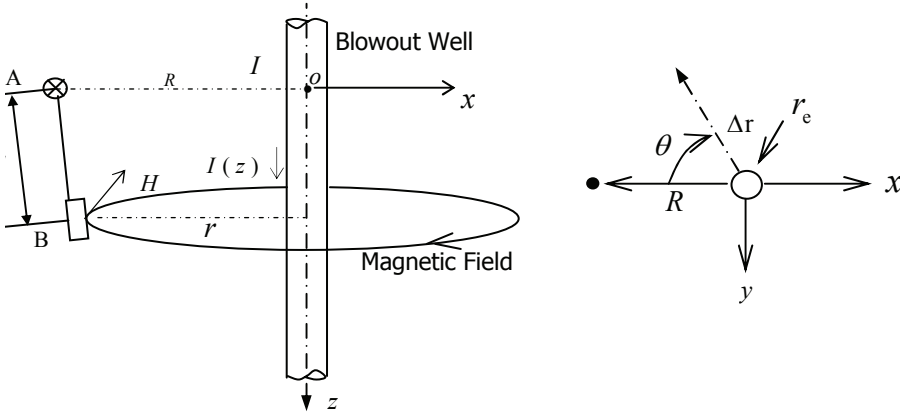


Figure 3: Response of casing in the blowout well to the current injected by single-electrode

The cylindrical coordinates are established such that the image position of the downhole electrode in the blowout well casing taken as the origin of coordinates, and the axis of the blowout well as the z-axis. The electric potential obeys the Laplace equation

$$\nabla^2 U = 0 \quad (5)$$

The electric potential must meet next boundary conditions: 1) at infinity, $U_\infty = 0$, 2) at $\Delta r = r_e$, U and $\partial U / \partial R$ is continuous [Jackson (1962); Abramowitz and Stegun (1965)]. When $\Delta r = 0$, assume that $r_e \ll R$, then

$$U(z) = \frac{I_0}{2\pi^2} \int_0^\infty \frac{K_0(\lambda R) \cos \lambda z d\lambda}{2\sigma_e + \frac{(\sigma_e - \sigma_c)(\lambda r_e)^2 \ln \lambda r_e}{2}} \quad (6)$$

So the electric field is obtained as

$$E(z) = \frac{I_0}{2\pi^2} \int_0^\infty \frac{uK_0(u) \sin(uz/R) du}{2\sigma_e R^2 + \frac{(\sigma_e - \sigma_c)(ur_e)^2 \ln(ur_e/R)}{2}} \quad (7)$$

Where $u = \lambda R$. Noting that E_{01} is known, so

$$\frac{E_1(z)}{E_{01}} = \frac{1}{\pi} \int_0^\infty \frac{uK_0(u) \sin(uz/R) du}{1 - \frac{1}{4} \frac{r_e^2}{R^2} u^2 \ln(ur_e/R)} \quad (8)$$

When $r_e \ll R$, the second term in the denominator of Eq.(8) is negligible as compared to unity, so Eq. (8) can be simplified as

$$\frac{E_1(z)}{E_{01}} = \frac{1}{\pi} \int_0^\infty uK_0(u) \sin(uz/R) du = \frac{z/R}{[1 + (z/R)^2]^{3/2}} \quad (9)$$

So under the condition of using the single-electrode, the current along the axis of blowout well can be obtained as:

$$I_1(z) = \frac{z/R}{[1 + (z/R)^2]^{3/2}} I_{\rho 1} = \frac{z/R}{[1 + (z/R)^2]^{3/2}} \cdot \frac{r_e^2}{4R^2} I_0 \quad (10)$$

As shown in Fig. 3, r is the distance between the casing of the blowout well and the sensor. We assume that the downhole electrode is located at point A and the sensor at point B in the relief well, that the points A and B are located in the same vertical plane, and that the spacing between these two points is d . The depth, inclination at point A and B respectively are given that $D_A, D_B, \alpha_A, \alpha_B$, and the average inclination of measuring well section is $\alpha_c = (\alpha_B + \alpha_A)/2$, the following equations are obtained

$$\begin{cases} R = r + d \sin \alpha_c \\ z = d \cos \alpha_c \end{cases} \quad (11)$$

Substituting Eq. (11) into Eq. (10), the current $I_1(z)$ on the casing in the blowout well a distance of r away is obtained

$$I_1(z) = \frac{d \cos \alpha_c}{[1 + (d \cos \alpha_c)^2]^{3/2}} \cdot \frac{r_e^2}{4(r + d \sin \alpha_c)^3} I_0 \quad (12)$$

By the Biot-Savart law, when using the detection tool based on a single-electrode, the strength of the magnetic field at the sensor in the relief well can be obtained as

$$H_1 = \frac{d \cos \alpha_c}{[1 + (d \cos \alpha_c)^2]^{3/2}} \cdot \frac{r_e^2}{4(r + d \sin \alpha_c)^3} \cdot \frac{\mu_0 I_0}{2\pi r} \quad (13)$$

From the upper equation, when the magnetic field at the sensor in the relief well is measured, the inverse relationship between the magnetic field strength H and the distance r can be used to estimate the distance from the relief well to the blowout well.

3.2 Current injected by a three-electrode array

To assure that the casing in the blowout well could concentrate as much current as possible, the three-electrode array is designed to be used in the detection tool. As shown in Fig. 4, the three-electrode array consists of three columnar metal electrodes: the main electrode A_0 is short, and is located in the middle of the three-electrode array, guard electrodes A_1 and A_2 are arranged to the upper and lower sides of the main electrode A_0 symmetrically. Insulating strips are located between three electrodes. When the measurement begins, a constant current I_0 is applied to the main electrode and an auxiliary current I_s of the same polarity is applied to the guard electrodes [Chu, Gao and Xiao (2007)]. At this time, the gradient of the electric potential along the three-electrode array is zero, so the current that flows out from the main electrode will not flow along the borehole axis and the main current I_0 is squeezed to roughly disk-shaped layer flow, thus more current is ensured to flow into the earth-formation and then gathered on the casing in the blowout well.

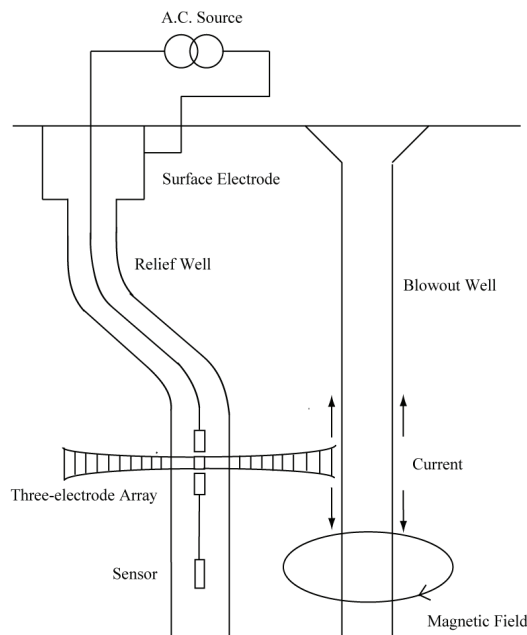


Figure 4: Working principle of detection tool based on three-electrode array

As shown in Fig. 5, assume that the three-electrode array is a line electrode without insulating strips, the current density j_0 is uniform, the total length of the three-electrode array is $2L_0$, the length of the main electrode is $2L$, and the radius of the three-electrode array is r_0 , which meets $r_0 \ll L_0$. The three-electrode array is located in the uniform formation with conductivity of σ_e [Zhang (1983)].

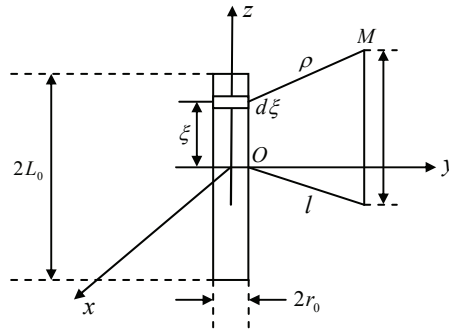


Figure 5: Current field calculation of line electrode

Taking the midpoint of the three-electrode array as the origin of coordinate system, whose z -axis is in accordance with the axis of the three-electrode array. Electric potential generated by current dI which flows out of infinitesimal $d\xi$ of the approximate line electrode is

$$dU = \frac{I_0}{8\pi\sigma_e L} \frac{d\xi}{\sqrt{l^2 + (z - \xi)^2}} \quad (14)$$

So the potential at a point M , generated by the three-electrode array is

$$U_2(l, z) = \frac{I_0}{8\pi\sigma_e L} \int_{-L_0}^{L_0} \frac{d\xi}{\sqrt{l^2 + (z - \xi)^2}} = \frac{I_0}{8\pi\sigma_e L} \ln \frac{\sqrt{l^2 + (z - L_0)^2} - (z - L_0)}{\sqrt{l^2 + (z + L_0)^2} - (z + L_0)} \quad (15)$$

If $z=0$, then

$$U_2(l, 0) = \frac{I_0}{8\pi\sigma_e L} \ln \frac{\sqrt{l^2 + L_0^2} + L_0}{\sqrt{l^2 + L_0^2} - L_0} \quad (16)$$

Thus the electric field with a distance l off the origin is as follows:

$$E_2(l, 0) = \frac{I_0}{4\pi\sigma_e L} \frac{L_0}{l\sqrt{l^2 + L_0^2}} \quad (17)$$

Similarly as shown in Fig. 3, the current concentrated on the blowout well casing can be expressed as

$$I_{\rho 2} = \sigma_c \cdot 2\pi r_c h_c E(r, 0) = \frac{\sigma_c r_c h_c I_0}{2\sigma_e L} \frac{L_0}{R\sqrt{R^2 + L_0^2}} = \frac{r_e^2 I_0}{4R\sqrt{R^2 + L_0^2}} \frac{L_0}{L} \quad (18)$$

Consider $L_0=0.8\text{m}$, $L=0.075\text{m}$, $I_0=20\text{A}$, as shown in Fig. 6, when the current I_0 injected by the downhole electrode is constant, the current concentrated on the blowout well casing injected by the three-electrode array is much higher than that injected by the single-electrode at the same distance from the relief well to the blowout well.

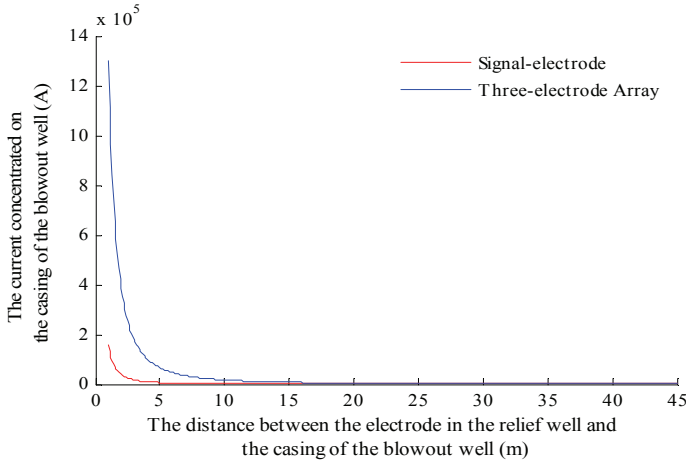


Figure 6: Comparison of current concentrated on the blowout well casing

It is known that the electric field along the z -axis of the blowout well casing is

$$E(z) = \frac{\partial U(z)}{\partial z} = \frac{I_0}{2\pi^2} \int_0^\infty \frac{uK_0(u) \sin(uz/R) du}{2\sigma_e R^2 + \frac{(\sigma_e - \sigma_c)(ur_e)^2 \ln(ur_e/R)}{2}} \quad (19)$$

When $R \gg L_0$, then

$$E_{02} = E(R, 0) \approx \frac{I_0 L_0}{4\pi \sigma_e L R^2} \quad (20)$$

Thus, by Eq. (9), we can obtain that

$$\frac{E_2(z)}{E_{02}} = \frac{L}{\pi L_0} \int_0^\infty uK_0(u) \sin(uz/R) du = \frac{L}{L_0} \frac{z/R}{[1 + (z/R)^2]^{3/2}} \quad (21)$$

So under the condition of using the three-electrode array, the current along the axis of the blowout well casing can be obtained as

$$I_2(z) = \frac{L}{L_0} \frac{z/R}{[1 + (z/R)^2]^{3/2}} I_\rho = \frac{z/R}{[1 + (z/R)^2]^{3/2}} \cdot \frac{r_e^2}{4R\sqrt{R^2 + L_0^2}} I_0 \quad (22)$$

Substituting Eq. (11) into Eq. (22), the current $I_2(z)$ on the blowout well casing related to the distance r is obtained

$$I_2(z) = \frac{d \cos \alpha_c (r + d \sin \alpha_c)}{(r^2 + 2rd \sin \alpha_c + d^2)^{3/2} [(r + d \sin \alpha_c)^2 + L_0^2]^{1/2}} \cdot \frac{r_e^2 I_0}{4} \quad (23)$$

The magnetic field strength at the sensor in the relief well can be obtained as

$$H_2 = \frac{d \cos \alpha_c (r + d \sin \alpha_c)}{(r^2 + 2rd \sin \alpha_c + d^2)^{3/2} [(r + d \sin \alpha_c)^2 + L_0^2]^{1/2}} \cdot \frac{\mu_0 r_e^2 I_0}{8\pi r} \quad (24)$$

4 Relative distance & direction from the relief well to the blowout well

The sensor mainly includes an accelerometer and a fluxgate magnetometer. The accelerometer is used to detect the gravitational field at the sensor, which combines with inclination data of the relief well to determine the orientation of the sensor. Similarly, the z -axis of fluxgate magnetometer is parallel to the axis of the sensor, and the x -axis and y -axis components are used to detect the magnetic field generated by the current on the casing in the blowout well. Signals detected by the sensor are transmitted to the ground, then the computational software will be used to calculate the relative distance and direction from relief well to blowout well [Kuckes (1987)].

Fig. 7 shows the computational model for determining the relative position of the relief well and the blowout well, vector n_1 is the direction along the axis of the blowout well, vector n_2 is the direction along the axis of the sensor, H is the magnetic field strength at the sensor generated by the current $I(z)$ on casing in the blowout well, H_p is the projection of H in the plane confirmed by the x -axis magnetic field component H_1 and the y -axis component H_2 , $H_p = (H_1^2 + H_2^2)^{1/2}$; H_d is the magnetic field component of H along the z -axis direction; H and vector r are located in the same plane and n_1 is perpendicular to this plane. As shown in Fig. 7, following equations can be obtained

$$\mathbf{H} = \mathbf{H}_p + \mathbf{H}_d \quad (25)$$

$$\mathbf{H}_d = -(\mathbf{H}_p \cdot \mathbf{n}_1) / (\mathbf{n}_1 \cdot \mathbf{n}_2) \quad (26)$$

$$\mathbf{r} / (\mathbf{r} \cdot \mathbf{r}) = (2\pi)(\mathbf{H} \times \mathbf{n}_1) / \mu_0 I \quad (27)$$

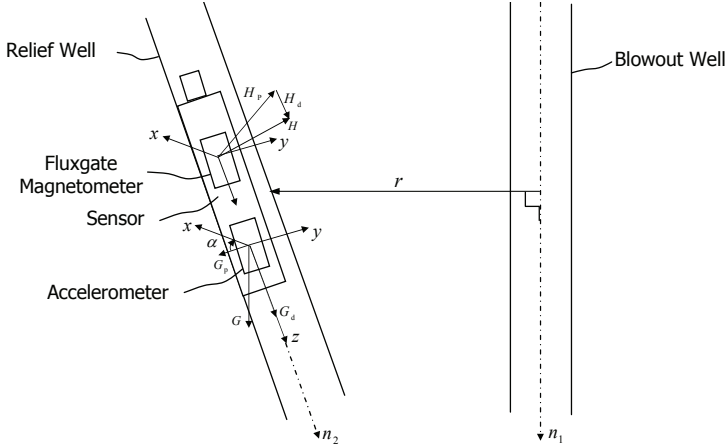


Figure 7: Calculation model for the relative position of relief well and blowout well

Therefore, after H_p is detected by the fluxgate magnetometer, substituting it into Eq. (25) ~ Eq. (27) to determine H and r uniquely, thus the distance between the relief well and the blowout well can be determined.

Similarly G_1 and G_2 are respectively the x -axis and the y -axis components of G_p , which is the component of gravitational vector G detected by the accelerometer in the sensor, $G_p=(G_1^2 + G_2^2)^{1/2}$. Angle α is the included angle of G_p and G_1 , angle β is the included angle of G_p and H_p . As shown in Fig. 7, it is obtained that $\cos(\alpha+\beta)=H_1/H_p$, $\sin(\alpha+\beta)=H_2/H_p$, $\cos\alpha=G_1/G_p$, $\sin\alpha=G_2/G_p$, so the cosine of angle β can be obtained

$$\cos\beta = \frac{G_1H_1 + G_2H_2}{G_1^2 + G_2^2} \cdot \frac{\sqrt{G_1^2 + G_2^2}}{\sqrt{H_1^2 + H_2^2}} \quad (28)$$

After substituting H_1 , H_2 , G_1 and G_2 as detected by the sensor into Eq. (28), we compute the angle β , and thus the direction from the relief well to the blowout well can be determined.

5 Case study and verification

According to the designed proposal of the exploration well LW21-1-1, the parameters of the earth-formation and casing are described as: $\sigma_e=1(\Omega\cdot\text{m})^{-1}$, $\sigma_c=10^7(\Omega\cdot\text{m})^{-1}$, $r_c=0.125\text{m}$, $h_c=0.0125\text{m}$, $\mu_0=4\pi\times 10^{-7}\text{T}\cdot\text{m}\cdot\text{A}^{-1}$. The magnetic field strength detected by the sensor is related to next parameters such as the current I_0 injected by

the downhole electrode, the spacing between the downhole electrode and the sensor, the length of the three-electrode array and the average inclination of the relief well.

5.1 Impact of the current magnitude injected by downhole electrode

Fig. 8 shows that when the distance of relief well and blowout well is the same, the larger the current injected by the downhole electrode, the stronger the magnetic field detected by the sensor. However, the skin effect of the casing limits the spread of the high-frequency alternating current into the earth-formation, and the current injected by the downhole electrode can't be infinite, so that the current injected by the downhole electrode is selected as being of high-amplitude (80A) and low-frequency (0.25Hz).

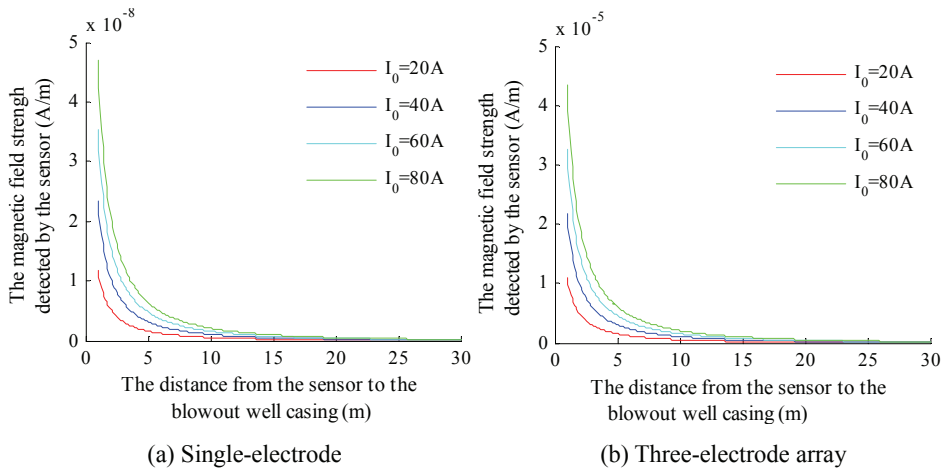


Figure 8: Impact of the current magnitude injected by the downhole electrode

5.2 Impact of spacing between the downhole electrode and the sensor

Fig. 9 shows that the larger the spacing between the downhole electrode and the sensor, the weaker the magnetic field strength as detected by the sensor. Because the magnetic field generated by flowing-up current concentrated on the blowout well casing has a bucking effect on the magnetic field detected by the sensor, in order to avoid the impact of the flowing-up current, the spacing is required to be at least 30m.

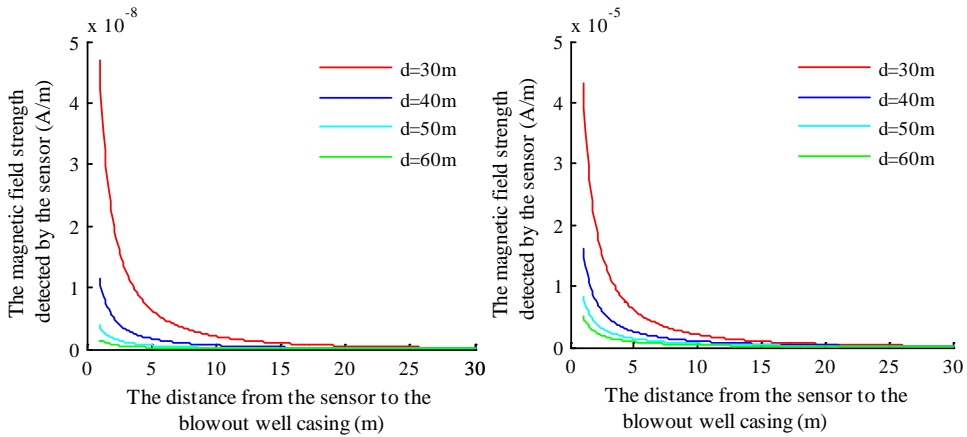


Figure 9: Impact of the spacing between the downhole electrode and the sensor

5.3 Impact of the length of the three-electrode array

Fig. 10 shows that when the length of three-electrode array is different, the curve representing the relationship between the magnetic field strength at the sensor and the distance from the relief well to the blowout well is almost the same, that is to say, the length of three-electrode array has little impact on the magnetic field strength detected by the sensor. Considering the difficulty in the level of tool production and field operation, combining the basic parameters of three-lateral-logging tool, the length of three-electrode array is selected as 1.6m.

5.4 Impact of the relief well inclination

Fig. 11 shows that the larger average inclination of the relief well, the weaker the magnetic field strength detected by the sensor. When the relief well is perpendicular to the blowout well, the magnetic field strength detected by the sensor is zero. When the axis of the relief well and the axis of the blowout well are in the same vertical plane, the direction of the magnetic field surrounding the casing in the blowout well will be perpendicular to the maximum sensitivity axis of the sensor, so the sensor has no signal output.

5.5 Comparison between single-electrode and three-electrode array

It is shown in Fig. 12 that when the basic parameters and the distance between the sensor and the blowout well casing are the same, the magnetic field strength detected by the detection tool based on three-electrode array is much larger than that based on single-electrode. Thus the detection tool based on three-electrode

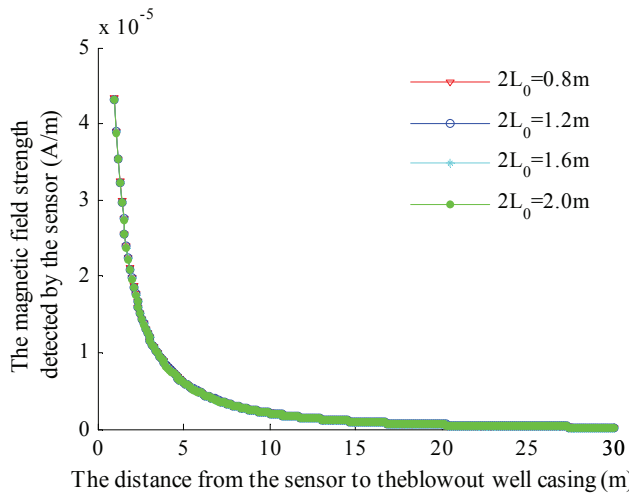


Figure 10: Impact of the length of three-electrode array

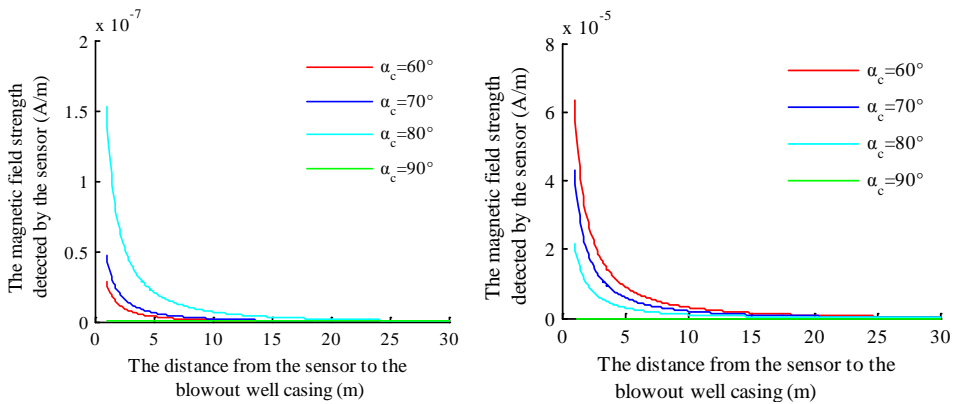


Figure 11: Impact of the deviation angle of the relief well

array is more conducive to its applications under actual working conditions.

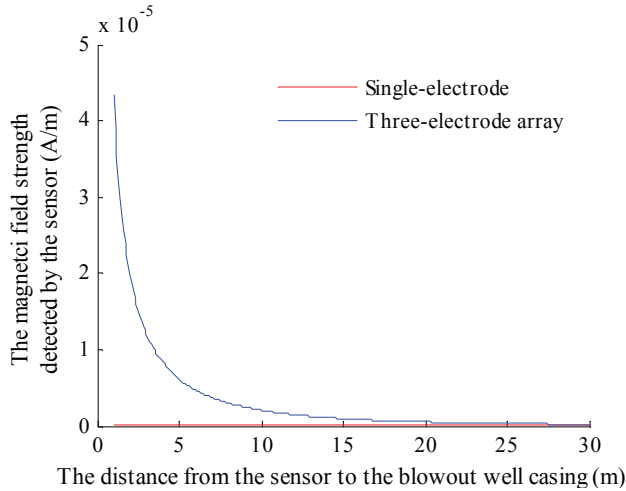


Figure 12: Comparison of magnetic field strength between single-electrode and three-electrode array

6 Conclusions

1. The method for computing the relative distance and direction from the relief the well to the blowout well, as presented here, can be used to develop the guidance tool for directional drilling of a relief well.
2. The spread and attenuation law of the current in the earth-formation, and in the casing of the blowout well, have been obtained by assuming the blowout well casing to be a cylindrical column of the earth-formation of an equivalent radius.
3. The spacing between the downhole electrode and the sensor is generally set as 30m, and the length of three-electrode array as 1.6m, which can meet the actual engineering requirements.
4. The computational formula is developed for using the magnetic field strength detected by the sensor to calculate the distance between the relief well and the blowout well. Moreover, the influences of some parameters, such as the length of three-electrode array, on the magnetic field strength detected by the sensor have been illustrated.

5. It is found by contrasting two kinds of detection tools that the detection tool based on three-electrode array is more immune to the sensitivity of the sensor, and thus is more conducive to its applications under actual working conditions.

Acknowledgement: The authors gratefully acknowledge the financial support of the Natural Science Foundation of China (NSFC, 51221003). This research was also supported by the other projects (Grant numbers: 2011ZX05009, 2010CB226703).

References

- Abramowitz, M.; Stegun, I.A.** (1965): Handbook of mathematical functions with formulas, graphs and mathematical tables. *Dover Publications Inc*, New York City.
- Arnwine, L.C.; Ely, J.W.** (1977): Polymer use in blowout control. *SPE 6835*.
- Bruist, E.H.** (1971): A new approach in relief well drilling. *SPE 3511*.
- Chen, X.B.; Zhao, G.Z.** (2009): Study on the transmitting mechanism of CSELF waves: response of the alternating current point source in the uniform space. *Chinese Journal of Geophysics*, vol.52, pp. 2158-2164.
- Chu, Z.H.; Gao, J.; Xiao, L.Z.** (2007): Geophysical logging method and principle (Rudin). *Beijing: Petroleum Industry Press*, pp.97-101.
- Diao, B.B.; Gao, D.L.** (2011a): Solenoid ranging system while drilling. *Acta Petrolei Sinica*, vol. 32, pp.1061-1066.
- Diao, B.B.; Gao, D.L.** (2011b): Adjacent well distance detection technology of the relief well and the blowout well. *The sixteenth national academic annual meeting of prospecting engineering technology(rock and soil drilling engineering)*, pp.192-196.
- Grace, R.D.; Kuckes, A.F.; Branton, J.** (1988): Operations at a deep relief well: the TXO Marshall *SPE 18059*
- Guo, Y.F.; Ji, S.J.; Tang, C.Q.** (2010): The relief well-the terminator of the Gulf oil leak. *Foreign Oilfield Engineering*, vol. 26, pp. 64-65
- Jackson, J.D.** (1962): Classical electrodynamics. *John Wiley and Sons Inc*, New York City.
- Kuckes, A.F.** (1982): Plural sensor magnetometer for extended lateral range electrical conductivity logging. *United States Patent*, US4323848, April, 1982.
- Kuckes, A.F.** (1987): Method for determining the location of a deep-well casing by magnetic field sensing. *United States Patent*, US4700142, October, 1987.

Kuckes, A.F.; Cornell, U.; Ritch, H.J. (1983): Successful ELREC logging for casing proximity in an offshore Louisiana blowout, *SPE 11996*, 1983.

Kuckes, A.F.; Hay, R.T.; McMahon, J. (1984): An electromagnetic survey method for directionally drilling a relief well into a blowout oil or gas well. *Society of Petroleum Engineers Journal*, pp.269-274.

Leraand, F.; Wright, J.W.; Zachary, M.B. (1990): Relief-well planning and drilling for a North Sea underground blowout. *SPE 20420*.

Morris, F.J.; Walters, R.L.; Costa, J.P. (1977): A new method of determining range and direction from a relief well to a blowout. *SPE 6781*.

Wang, D.G.; Gao, D.L. (2008): Study of magnetic vector guide system in tubular magnet source space. *Acta Petrolei Sinica*, vol. 20, pp. 608-611.

Zhang, G.J. (1983): Electrical logging (Rudin). *Beijing: Petroleum Industry Press*, pp.45-50.

